A New Modular Approach to Nanoassembly: Stable and Addressable DNA Nanoconstructs *via* Orthogonal Click Chemistries

Simon R. Gerrard,[†] Claire Hardiman,[†] Montserrat Shelbourne,[†] Iris Nandhakumar,[†] Bengt Nordén,[‡] and Tom Brown[†,*]

[†]School of Chemistry, University of Southampton, Highfield, Southampton, SO17 1BJ. U.K. and [‡]Department of Chemical and Biological Engineering, Chalmers University of Technology, Gothenburg, S41296, Sweden

ABSTRACT

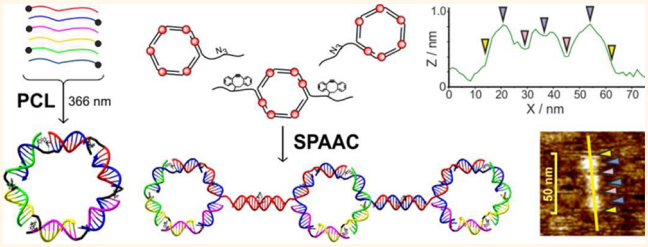

Thermodynamic instability is a problem when assembling and purifying complex DNA nanostructures formed by hybridization alone. To address this issue, we have used photochemical fixation and orthogonal copper-free, ring-strain-promoted, click chemistry for the synthesis of dimeric, trimeric, and oligomeric modular DNA scaffolds from cyclic, double-stranded, 80-mer DNA nanoconstructs. This particular combination of orthogonal click reactions was more effective for nanoassembly than others explored. The complex nanostructures are stable to heat and denaturation agents and can therefore be purified and characterized. They are addressable in a sequence-specific manner by triplex formation, and they can be reversibly and selectively deconstructed. Nanostructures utilizing this orthogonal, chemical fixation methodology can be used as building blocks for nanomachines and functional DNA nanoarchitectures.

KEYWORDS: DNA nanotechnology · photochemical cross-linking · copper-free click · orthogonal chemical fixation

DNA is an exciting material for nanotechnology applications. Machines and structures of the kind already constructed from DNA[1,2] would be impossible to make with other materials, and the complexity of DNA-based nanostructures is beyond that of those produced by any other method. One approach that has been particularly effective is DNA origami.[3,4] This method typically uses a biological material, bacteriophage M13 DNA, which is a convenient nanobuilding material. Large numbers of short oligonucleotide staples promote folding of the M13 DNA into predetermined shapes such as DNA smilies[3] and three-dimensional nanoboxes.[5] DNA origami has the advantage of simplicity; the structures are intramolecular in nature, so careful control of the stoichiometric ratios of staple strands and M13 DNA is unnecessary. However, this is not a true bottom-up approach, and it is not applicable to objects and machines at the most demanding low end of the nanoscale, which bridges the gap between supramolecular chemistry and nanotechnology. This is a domain more suited to approaches that utilize chemically synthesized DNA, which can be produced with high efficiency on a large scale. We are currently developing methods to target this space that involve the assembly of densely packed and uniquely addressable DNA nanostructures.[6] Our approach allows the site-specific incorporation of a wide variety of chemical modifications to create information-rich nanoconstructs that cannot be obtained by conventional thermochemical,[7] electron-beam,[8] photo,[9] or dip-pen nanolithography.[10,11] Nanoassembly by synthesis is a valuable technique for the future, and such nanoconstructs are themselves key materials for building larger and more complex structures.

The integrity of DNA nanoconstructs assembled by hybridization relies on the selectivity of Watson–Crick base pairs and on the stability derived from hydrogen bonding and base stacking.[12] There are difficulties in manipulating such materials, as these interactions are dynamic and reversible. Consequently, DNA nanoconstructs are fragile, difficult to purify, and unsuitable for use as robust building blocks

* Address correspondence to tb2@soton.ac.uk.

Received for review August 7, 2012 and accepted September 14, 2012.

Published online September 18, 2012
10.1021/nn3035759

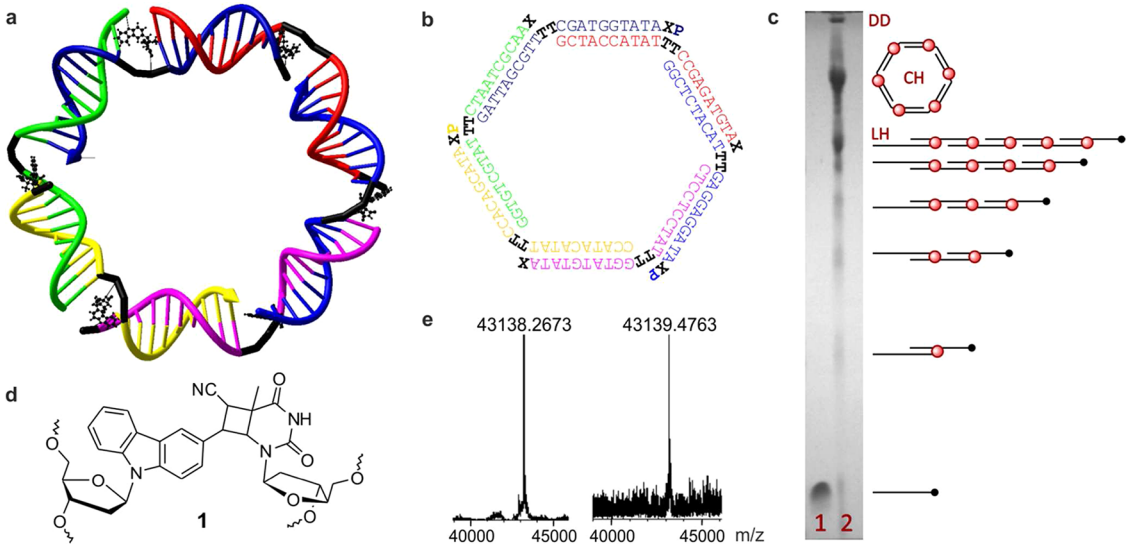

Figure 1. Photo-cross-linked hexagon structure and assembly. (a) Representation of a photo-cross-linked hexagon. ^{CNV}K-T cross-linked dinucleotides and TT hinges are shown in black. (b) Hexagon sequences and secondary structure: X = ^{CNV}K, P = 3′-propanol, TT = single-stranded hinge. (c) Analytical denaturing polyacrylamide gel (10%) of construction of unmodified hexagon (5 μM, containing ODN-1 to ODN-6, irradiated at 20 °C; ODN = oligodeoxynucleotide). Lane 1: un-cross-linked, lane 2: photo-cross-linked. LH = linear hexamer, CH = cyclic hexamer (hexagon), DD = dodecamer. Red circles indicate photo-cross-links, black dots indicate un-cross-linked ^{CNV}K nucleotides. See Supporting Figure S1 for full image. (d) Proposed structure of ^{CNV}K-T cross-linked dinucleotide 1.[24] (e) Electrospray MS spectra of purified cyclic hexamer (hexagon, CH, left) and linear hexamer (LH, right) (negative mode). Calcd mass (hexamer): 43140.893, found: 43138.267 (CH), 43139.476 (LH).

for the assembly of higher order structures.[13] To address this problem, enzymatic ligation has been used for their fixation,[14,15] but it is limited to nicks in the backbone of linear sequences, is hindered by densely packed and constrained DNA helices, and is not amenable to large-scale synthesis. We have previously employed an alternative chemical solution, click ligation, using the CuI-catalyzed alkyne−azide cycloaddition reaction (CuAAC), which enabled the synthesis of a robust, hexagonal, double-stranded DNA nanoconstruct.[16] A different strategy has also been used that involves soaking of prehybridized DNA nanostructures with a solution of 8-methoxypsoralen.[17,18] Subsequent UV irradiation promotes a series of [2+2]-cycloaddition reactions between the intercalated psoralen molecules and thymine bases at TA steps in the DNA. This chemistry is difficult to control, as it requires insertion of an external agent into DNA, and induces a large perturbation in the local B-DNA secondary structure.[19] Anthracene photodimerization has also been employed for reversible DNA duplex cross-linking,[20] and there are examples of photochemical ligation using 5-carboxy- and 5-carbamoylvinyl-dU.[21] We now report the fixation of small, discrete pseudohexagonal nanostructures of ∼9 nm diameter by photochemical interstrand cross-linking (PCL) using a 3-cyanovinylcarbazole moiety (^{CNV}K) integrated into the DNA chain during solid-phase synthesis. It intercalates into the duplex, and on UV irradiation at 366 nm, the cyanovinyl group undergoes a [2+2]-cycloaddition reaction with the C5−C6 double bond of a pyrimidine base in the opposite strand (Figure 1d, Supporting Information S1.1.2).[22−28] The ^{CNV}K moiety has recently been used in the formation of non-modified, periodic 2D arrays of DXAB DNA tiles, *via* fixation of simple, sticky-end overlaps of tiles that are otherwise non-fixed.[29] Here we have utilized ^{CNV}K in a significantly more demanding task: to construct the smallest possible, entirely chemically fixed, planar pseudohexagonal DNA nanoconstruct *via* six simultaneous photochemical cross-linking reactions. The construct was synthesized from six short, easily purified oligonucleotides, with superior efficiency and yield compared with our previous method[16] (Supporting Figure S1) and with more precision than other photochemical methodologies. We have also constructed a simpler pseudohexagonal structure (*vide infra*) *via* just two PCL reactions. In contrast to our previous CuAAC ligation methodology,[16] this photochemical fixation technique forms rigid inter-base cross-links within the duplex itself, rather than *via* long linkers in the major groove, and imparts significant extra duplex stabilization.[30] Moreover, the ^{CNV}K moiety is easily incorporated during oligonucleotide synthesis instead of *via* postsynthetic labeling, and the fixation technique requires a substantially shorter reaction time (1 h *vs* 24 h).

These photochemically cross-linked DNA nanoconstructs can be purified by denaturing polyacrylamide gel electrophoresis (PAGE) and characterized by mass spectrometry. They are stable to heat and can be used in the controlled assembly of larger structures, which in turn can be fixed using an orthogonal chemical procedure, the ring-strain-promoted alkyne−azide cycloaddition (SPAAC) reaction,[31] which has hitherto not been

used in fixation of DNA nanostructures, or in conjunction with photochemical fixation methods.

RESULTS AND DISCUSSION

Photo-cross-linked Hexagon Design and Assembly. The basic building block for large nanoconstructs, a monomeric, cyclic DNA structure,[6,16] was assembled from six 23-mer/24-mer oligonucleotides, each involved in the formation of two sides of a hexagon, each side being 10 base pairs in length (one helical turn of DNA) (Figure 1b). The oligonucleotides were synthesized by standard solid-phase phosphoramidite chemistry, incorporating the ^{CNV}K nucleotide[24] at the 5′-end (ODN-2, ODN-4, ODN-6; ODN = oligodeoxynucleotide) or at the 3′-end (ODN-1, ODN-3, ODN-5) using a 3′-propanol-modified solid support (oligonucleotide design, sequences, and ESMS data in Supporting Information S1.1.1−S1.1.2). Flexible, single-stranded TT hinges/nodes were placed at the vertices of the hexagon (at the center of each oligonucleotide) to enable cyclization of such small nanostructures, unlike the non-DNA, terphenyl-based nodes of Sleiman *et al.* for example,[32−34] and ^{CNV}K nucleotides were placed adjacent to the vertices for cross-linking with the thymine base of the neighboring AT base pair or the hinge. The oligonucleotide sequences were carefully designed to ensure that only the desired hexamer, and no branched or alternative cyclic structures, could form. Six PCL reactions were carried out simultaneously upon UV irradiation (365 nm), to produce a covalently locked, cyclic nanostructure, each side consisting of a short (10 bp), stable duplex with one covalently cross-linked end (Figure 1). The precise positioning of the ^{CNV}K nucleotides ensures that only the desired cross-linking can occur.

PCL hexagons were synthesized by several methods: "one-pot" construction, or *via* trimers, and under different annealing/irradiation protocols (Supporting Information S1.1.4). The simplest method involved annealing all six oligonucleotides slowly from 85 °C to room temperature, followed by a short incubation. Samples were UV-irradiated while cooling on ice (365 nm), desalted, lyophilized, then purified by denaturing PAGE. Figure 1c shows the crude reaction mixture for construction of the unmodified cyclic hexamer. The reaction affords the hexagon (cyclic hexamer, CH), the uncyclized hexamer (linear hexamer, LH), and a small quantity of dodecamer (DD). It proceeds in greater yield and with fewer byproducts than the analogous CuAAC click fixation strategy we have previously described.[16] The two bands for CH and LH are clearly distinct from smaller constructs, CH showing lower electrophoretic mobility than the linear construct as previously observed,[16] rationalized by a greater degree of interaction with the polyacrylamide gel matrix (also Supporting Figure S1). The topology of large DNA structures is known to significantly influence mobility during PAGE.[35] Hexamers CH and LH were isolated pure, in typical yields of 14−16% and 7−13%, respectively, after a single denaturing gel purification, an excellent result when the efficiency of hybridization, six simultaneous PCL reactions, and extraction from gel are all taken into account. The yield of LH depends on efficiency of cyclization during cooling and of the PCL reaction itself. Slowing the rate of cooling over the melting transition temperature range appeared to promote cyclization, thus favoring CH over LH, although this process is controlled by a combination of factors. The high NaCl concentration (500 mM) is necessary to shield negative charges for efficient hybridization/cyclization.

To prove that LH was not an inactive (dead-end) linear intermediate, the construct was isolated from the gel, reannealed, then irradiated for 30, 60, and 90 min. This resulted in partial conversion to the cyclic product CH, and the yield increased slightly with prolonged irradiation (34.8%, 30 min; 44.4%, 90 min). No UV-induced degradation was observed (Supporting Figure S2). The ability to convert LH into CH, which has a lower electrophoretic mobility, both of which have the same mass, confirms the cyclic nature of the construct. A pseudohexagonal structure was also constructed, from two ^{CNV}K-modified 70-mer oligonucleotides (ODN-7, ODN-8, Supporting Figures S3, 4), *via* only two photochemical cross-linking reactions. The cyclic structure (cyclic dimer, CD) is formed easily in high yield, in preference to the linear structure (linear dimer, LD), with photo-cross-linking at 20 or 0 °C. This is a simpler strategy, but it requires much longer oligonucleotides and it does not rigorously test the efficiency of multiple, simultaneous cross-linking reactions.

Single-Hexagon Spectroscopic Studies. Spectroscopic methods were used to investigate the properties of the fixed cyclic construct. Melting studies were performed on the purified, unmodified "fixed" hexamers (LH and CH) and the unfixed hybridized structure, using SyBr Green I. This dye becomes strongly fluorescent only upon intercalation into double-stranded DNA and enables the duplex melting temperature (T_m) to be determined by monitoring of fluorescence. Fluorescence melting was first conducted using 48 equiv of SyBr Green I per construct (8 molecules per hexagon side), in sodium phosphate buffer (500 mM NaCl), with 0%, 20%, and 40% formamide (v/v) (Figure 2b, Supporting Figure S5). The non-cross-linked, hybridized structure denatures with an approximately linear melting transition from 37 to 56 °C. This results from the superposition of melting curves of all six duplexes in the hexagon (with different individual melting temperatures). Addition of formamide destabilizes the unfixed hexagon such that little or no hybridization occurs. The chemically fixed PCL constructs (LH, CH), however, possess greatly enhanced stability, with significant duplex present at 50 °C in the presence of 20%

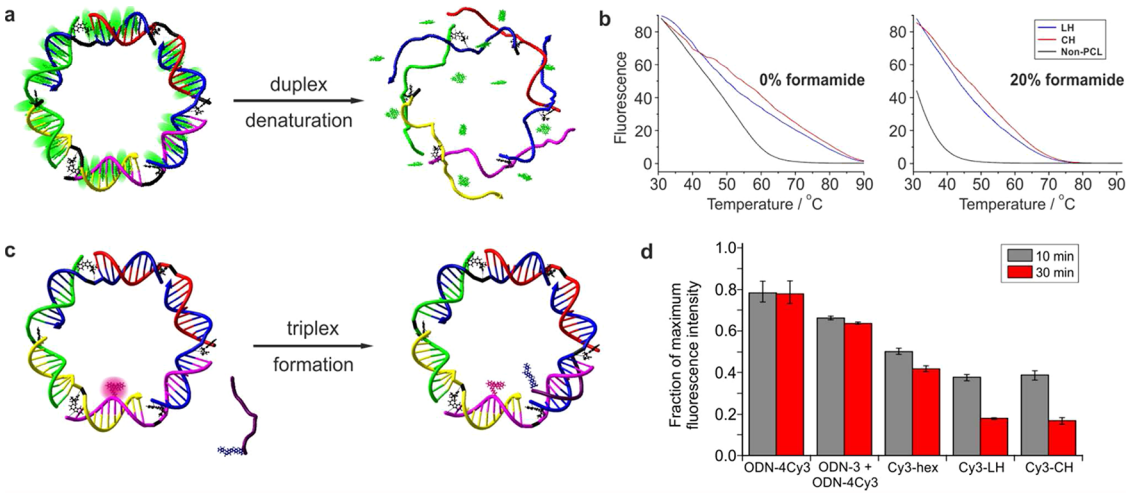

Figure 2. Fluorescence spectroscopic studies on single PCL hexagon. (a) PCL hexagon denaturation, indicating loss of fluorescence as intercalated SyBr Green I molecules dissociate; denatured hexagon remains intact due to covalent cross-links. (b) Fluorescence melting analysis of unmodified hexamer (non-PCL, LH, and CH) using the fluorescent double-stranded DNA intercalator SyBr Green I (48 equiv per construct) (Supporting Figure S5 and Table S1) with 0% and 20% v/v formamide. The PCL hexagon can melt but not disassemble under denaturing conditions, and the cross-links significantly enhance duplex stability. (c) Hexagon triplex formation, indicating loss of fluorescence of Cy3 dye on binding of BHQ-2-labeled triplex-forming oligonucleotide (TFO-1). (d) Fluorescence intensity, as a fraction of maximum fluorescence intensity, at 10 and 30 min after addition of TFO. Significant fluorescence quenching and therefore efficient triplex formation occurs only for chemically fixed constructs Cy3-LH and Cy3-CH (Supporting Figure S7).

formamide denaturing agent (Figure 2a,b, Supporting Table S1).

Melting profiles for CH and LH are similar, exhibiting several overlapping transitions. It is important to emphasize that the PCL constructs cannot be destroyed by heating and/or denaturation with formamide; the hexagon is covalently fixed at each vertex; therefore although melting of each side can occur, the nanoconstructs remain intact. These experiments were also conducted for LH and CH using only 18 equiv of SyBr Green I (3 molecules per hexagon side), at variable construct concentrations, to reduce the general stabilizing effect due to fluorophore intercalation, and similar melting profiles were observed (Supporting Figure S6 and Table S2).

The photo-cross-linked hexagon is also addressable in a sequence-specific manner by triplex-forming oligonucleotides (TFOs), allowing targeting with oligonucleotides containing various functionalities. A hexagon was constructed using ODN-1, 2, 3, 5, and 6 and a Cy3-labeled analogue of ODN-4 (ODN-4Cy3), placing the Cy3 dye in the center of one side, adjacent to the triplex-binding site (Figure 2c,d, Supporting Information S1.1.4; the Cy3 hexagon was also constructed from two trimers, Supporting Information S1.1.4). This site was targeted using a BHQ-2-labeled TFO (TFO-1); the BHQ-2/Cy3 pair is suitable for through-space quenching. Fluorescence triplex targeting experiments were conducted using a 10:1 ratio of TFO to nanoconstruct (Figure 2d, Supporting Figure S7). Significant fluorescence quenching due to triplex formation was observed for the PCL constructs. The triplex melting temperature (T_m) is close to the midpoint of the duplex melting transition (Figure 2b), suggesting the TFO dissociates cooperatively with the duplex (Supporting Table S3). Fixation stabilizes the duplex target such that the TFO is able to bind efficiently; without fixation, little triplex formation is observed, and consequently there was minimal fluorescence quenching. Fluorescence melting studies on the non-cross-linked system (Cy3-hex) also indicated a weak triplex melting transition and poor fluorescence quenching (Supplementary Figure S8). These results demonstrate that a compact, constrained, stabilized nanostructure can be addressed by triplexes and that chemical fixation is vital for efficient TFO binding.

Modular Construction of DNA Nanostructures. The programmed assembly of modular networks using these hexagonal building blocks requires single-stranded, sticky ends for connecting the modules (Figure 3a). In order to "fix" higher order structures, we chose an orthogonal chemical method, the ring-strain-promoted alkyne−azide cycloaddition reaction, an efficient click reaction that utilizes the inherent ring strain in cyclooctyne as a source of energy. Recently, we established that very fast and efficient templated DNA ligation can be achieved by reaction between oligonucleotides functionalized with dibenzocyclooctyne (DIBO[36]) and azides.[37] The fused benzene rings impart significant ring strain and also enhance reactivity due to their electron-withdrawing properties.[38] More recently, we utilized DIBO in interstrand cross-linking of simple DNA duplexes.[39] The cross-linking reactions were fast and highly efficient.

Hexagonal modules were constructed with one or two branches, comprising one of two complementary

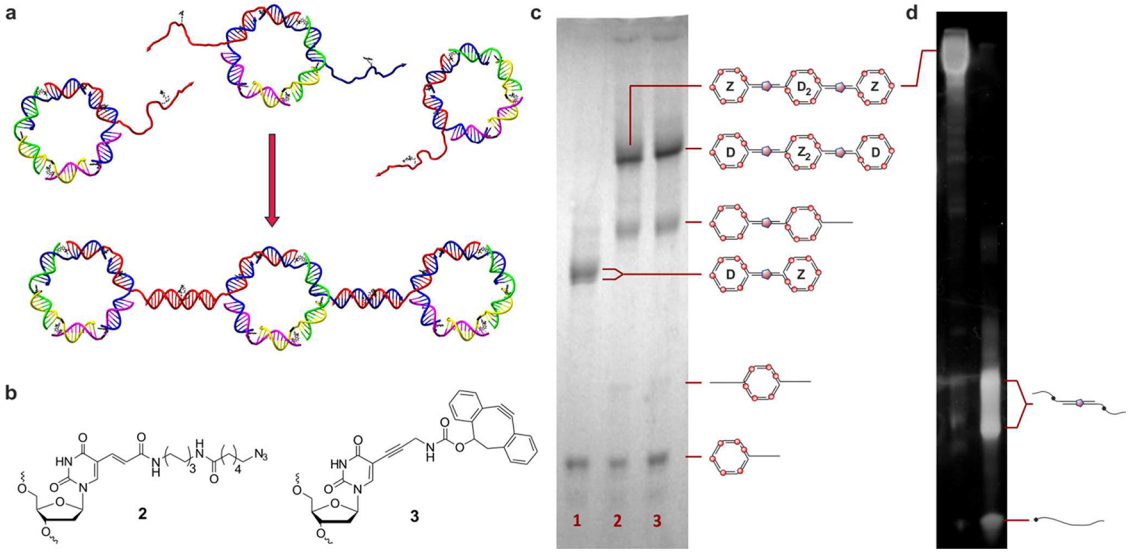

Figure 3. Branched hexagons, modular construction of copper-free click-fixed nanoarrays, and photolytic deconstruction. (a) Formation of hexagon trimer: hybridization of branches followed by rapid, templated ring-strain-promoted click fixation. (b) Azidohexanoyl-labeled amino-C6-dT nucleoside, 2, and 5-propargyl-DIBO-dU nucleotide, 3. (c) Preparative denaturing polyacrylamide gel (5%) of dimeric and trimeric nanostructures. Lane 1: construction of dimer (present as two close running bands due to DIBO-azide triazole adduct isomeric forms, Supporting Figure S9). Lane 2: construction of trimer 1 (two Z-CH hexagons and one $DIBO_2$-CH hexagon). Lane 3: construction of trimer 2 (two DIBO-CH hexagons and one Z_2-CH hexagon). See Supporting Figure S10 for full image. (d) Analytical denaturing polyacrylamide gel (6%) of trimer deconstruction by irradiation. Trimer 1 (left), trimer 1 deconstruction (right), showing SPAAC duplex (ODN-1−2) and individual oligonucleotides ODN-3−ODN-6, formed due to destruction of PCLs. See Supporting Figure S11 for full image. Red circles indicate photo-cross-links, black dots indicate uncross-linked ^{CNV}K nucleotides, and pentagons indicate SPAAC cross-links. Z and D indicate azide-modified and DIBO-modified hexagons Z-CH and DIBO-CH, respectively. Z_2 and D_2 indicate diazide- and di-DIBO-modified hexagons Z_2-CH and $DIBO_2$-CH, respectively.

sequences only (Figure 3a,b). These were designed to form a dimer and trimers (or to oligomerize), depending on how they are combined. Both DIBO and azide residues are attached *via* the 5-position of a thymidine nucleotide and are therefore located in the major groove. When hybridized, these moieties are brought adjacent to each other, enabling spontaneous cross-linking. The branch was designed to be 20 nucleotides long with a 4T "hinge" to enable adequate length and flexibility for duplex stability when hybridized, while remaining short enough to maintain suitable structural rigidity of the resultant oligomer. It was also necessary to move the position of the photo-cross-link away from the branch point (vertex) to the center of the side in azide-modified oligonucleotide ODN-2Z and DIBO-modified oligonucleotide ODN-2DIBO, to enable cyclization of the branched construct. The branch appears to cause fraying of the duplex at the vertex, thus preventing the ^{CNV}K moiety from intercalating and forming the photo-cross-link. Consequently, when ^{CNV}K was placed at the vertex, little or no cyclization occurred (data not shown). PCL hexagons were lyophilized individually, then combined in 0.6 M NaCl (5 μM). The cross-linking reactions were simply incubated at room temperature for at least 1 h, during which time the desired dimer, trimer, or oligomer formed in high yield (Figure 3c, Supporting Figure S10). It was important not to lyophilize azide- and DIBO-modified hexagons together, as high concentration can cause non-templated SPAAC reactions to occur.

Higher order dimeric, trimeric, and oligomeric nanostructures were successfully purified by denaturing PAGE (Figure 3c, Supporting Figure S10), highlighting their excellent stability. Surprisingly, the normally highly efficient CuAAC click reaction was very inefficient in this context compared to SPAAC. No cross-linking was observed between azide-modified branched hexagon Z-CH and the terminal alkyne-modified hexagon analogue of DIBO-CH (K-CH) in the copper-catalyzed reaction (Supporting Information S1.1.7, Supporting Figure S12b), despite efficient hybridization (Supporting Figure S13). Only moderate cross-linking was observed between oligonucleotides ODN-2Z and the terminal alkyne analogue of ODN-2DIBO (ODN-2K) (Supporting Figure S12a). This is further evidence of the remarkable efficacy of the DNA-templated SPAAC fixation method, which works well even under these demanding conditions, where CuAAC fails.

AFM tapping mode imaging (Figure 4a, Supporting Figure S14) and cross-sectional analysis of the purified dimeric construct show pairs of cyclic structures, consistent in size and shape with the hexagon dimer structure. Both methods of trimer formation (trimer 1: 2 × Z-CH + $DIBO_2$-CH; trimer 2: 2 × DIBO-CH + Z_2-CH) a4fforded predominantly linear trimeric structures as designed (Figure 4b, Supporting Figures S15, 16).

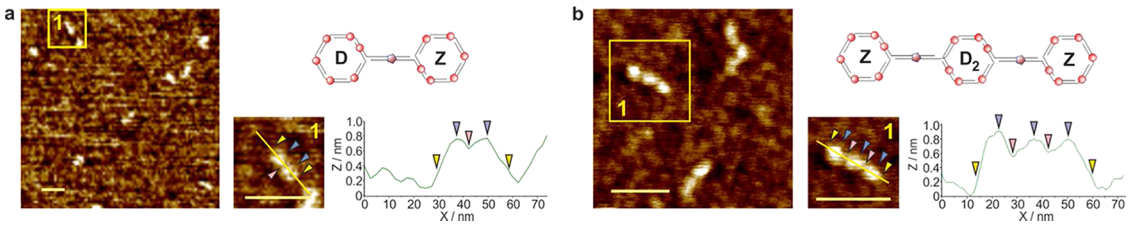

Figure 4. Analysis of dimeric and trimeric DNA hexagon nanostructures. AFM images and cross-sectional analyses. (a) Hexagon dimer. (b) Hexagon trimer 1. Red circles indicate photo-cross-links, and pentagons indicate SPAAC cross-links. Z, D, and D_2 indicate Z-CH, DIBO-CH, and $DIBO_2$-CH, respectively. Scale bars: 50 nm. Yellow, blue, and pink arrows indicate the ends, peaks (hexagon center), and troughs (interhexagon duplex) of oligomers, respectively. Nanostructure dimension measurements are consistent with calculated values (Supporting Figures S14–15). See Supporting Figure S16 for trimer 2 AFM image analysis.

DNA structure height was 0.7–0.9 nm, consistent with that of a single duplex imaged in tapping mode in air.[40]

Oligomers (up to 300 nm) and a cyclic oligomer were also formed simply by incubation of Z_2-CH and $DIBO_2$-CH in solution at room temperature and were isolated by gel purification. Individual hexagons in these oligomers could be distinguished and counted (Supporting Figure S17). Longer oligomers/polymers of 150–400 nm or greater in length were obtained by a two-step anneal process (Supporting Information S1.1.5, Supporting Figures S18, 19). All hexagons and higher order structures, including the longest oligomers, were completely soluble in water or aqueous buffer.

In addition to nanostructure stability, addressability, and orthogonality of cross-linking methods, reversibility is also a valuable feature of this photochemical cross-linking method. Networks and arrays may be constructed and then selectively deconstructed by irradiation at 312 nm, while leaving nonphotochemical cross-links and the constituent oligonucleotides undamaged. To demonstrate this, we irradiated trimer 1 in 50% aqueous formamide at 302 nm (UV transilluminator) at room temperature. Irradiation for 5 min was sufficient to destroy all photochemical cross-links (Figure 3d, Supporting Figure S11), leaving SPAAC cross-links and the oligonucleotides intact. The SPAAC cross-linked duplex product runs as two distinct bands on denaturing polyacrylamide gel due to triazole regioisomers as previously described (Supporting Figure S9). The separation is far greater than for the hexagon dimer (Figure 3c), as expected for a small duplex.

CONCLUSION

The combination of photochemical and SPAAC interstrand cross-linking is a powerful and versatile chemical tool for formation of high-order DNA nanostructures. This two-pronged approach allows for construction and purification of discrete nanostructure units, which may be easily combined for controlled assembly of larger nanoconstructs. These chemically fixed DNA structures are stable to heat and denaturing agents, can be addressed in a sequence-specific manner with DNA triplex forming oligonucleotides, and can be selectively deconstructed by irradiation. This photochemical cross-linking method should also be applicable to fixation of DNA origami *via* ^{CNV}K-modified staple strands, due to its high efficiency in such a sterically demanding environment. The combination of reversible and irreversible orthogonal fixation strategies and robust, specific building blocks leads the way toward clearly defined, designer, functional DNA nanoarchitectures with a high density of information storage (*e.g.*, triplex binding sites, restriction enzyme digestion sites, incorporation of dyes, biotin, or other chemical moieties). There are exciting prospects for this methodology in DNA nanotechnology applications, such as dynamic DNA strand replacement reactions,[41] and applications in DNA nanodevices,[1,42,43] DNA-templated polymer synthesis,[44,45] and the developing field of DNA nanobioelectronics.[46,47]

METHODS

Buffer Systems. 1× TBE buffer: 89 mM Tris, 89 mM boric acid, 3.2 mM EDTA, pH 8. AFM loading buffer: 10 mM HEPES, 5 mM $NiCl_2$, pH 7.58.

Gel Electrophoresis. Analytical and preparative denaturing polyacrylamide gels (5–10%) containing 7 M urea were run in 1× TBE buffer for 1.5–2.5 h at 20 W and visualized by UV shadowing or by transillumination (302 nm) after staining with SyBr Gold nucleic acid stain (Invitrogen).

Fluorescence Nanoconstruct Melting. Fluorescence melting was performed on a Roche LightCycler 1.5 instrument in LightCycler glass capillaries (20 μL) in triplicate using Roche LightCycler software v3.5.[48] Samples were excited at 488 nm, and change in fluorescence was monitored at 520 nm. For each experiment, 4.5 μL of a 5 μM master solution of the unlabeled PCL hexamer or a combination of 4.5 μL of 5 μM master solutions of ODN-1–ODN-6 was lyophilized. Samples were resuspended to a concentration of 0.25 μM in 90 μL of a solution containing 27.44 μL of 20× SyBr Green I solution (dilution from 10 000× concentrate in DMSO with 10 mM sodium phosphate, 500 mM NaCl buffer, pH 7.0) and either 62.56 μL of buffer, 44.56 μL of buffer + 18 μL of formamide, or 26.56 μL of buffer + 36 μL of

formamide to give solutions containing 12 μM SyBr Green I (approximately 48 equiv per construct) and 0, 20, and 40% v/v formamide. Samples were denatured by fast heating to 95 °C and held at 95 °C for 5 min. Samples were annealed by slow cooling to 30 at 0.2 °C min^{-1}, incubated at 30 °C for 60 min, then melted by slow heating to 95 at 0.2 °C min^{-1}, followed by incubation at 95 °C for 10 min to equilibrate. Fluorescence was measured at 1 °C intervals. SyBr Green I concentration for commercially available 10 000× concentrate in DMSO has been determined to be approximately 19.6 mM.[49]

Triplex Nanoconstruct Targeting. Fluorescence measurements were performed in triplicate on a Perkin-Elmer LS 50 B luminescence spectrometer, in a Hellma SUPRASIL synthetic quartz fluorescence cuvette (10 mm path length), using the "Intensity" and "TimeDrive" functions in FLWinLab software, in single-read mode. Samples of each target were suspended in buffer (10 mM sodium acetate, 200 mM NaCl, pH 5.5) to a concentration of 16 pmol in 158 μL, and fluorescence emission was measured. Samples were excited at 555 nm, and emission was monitored at 568 nm with excitation/emission slit widths of 7.0/8.0 nm and 5 s average integration time, at 20 °C (average of 6 sequential readings, taken after equilibration). The fluorescence time course was started on addition and mixing of TFO (160 pmol in 2 μL), measuring fluorescence at 60 s intervals with the above settings, for 30 min. Final concentration: 0.1 nM Cy3-target, 1 nM TFO. Preparation of non-photo-cross-linked samples is described in the Supporting Information, S1.1.10.

Atomic Force Microscopy. AFM images were acquired on a Multimode AFM with a Nanoscope III controller in tapping mode. Imaging was performed in air. Samples were dissolved to a concentration of 5 nM for dimer and trimers. Concentration of oligomer was less than 5 nM (varied depending on oligomer length). A volume of 10 μL of sample in AFM loading buffer was applied to a freshly cleaved mica surface and incubated for 5−8 min (typically 6 min). Unadsorbed material and salt were washed off gently with ultrapure water from an Elga UHQ-II water purification system (18.2 MΩ·cm resistivity). The surface was dried immediately under compressed air. Force modulation point probes (Nanoworld, k = 2.8 N m^{1-}) were used, with a resonance frequency of 75 kHz and typical radius of curvature of less than 8 nm. The amplitude set point was varied from 0.38 to 0.50 V, with a scanning frequency of 1.5−2.4 Hz. AFM raw data were processed using Bruker NanoScope Analysis 1.4 software and leveled using a third-order plane fit, and cross-sectional analysis and nanostructure measurements (average of 20 individual constructs) were obtained using the freeware program WSxM (Nanotec Electronica).[50]

Conflict of Interest: The authors declare no competing financial interest. S.R.G. helped carry out AFM imaging, planned and carried out the experiments, and prepared the manuscript. C.H. carried out initial studies into PCL hexagon construction and purification. M.S. contributed 5-propargyl-DIBO-dU monomer and advice on SPAAC experiments. I.N. carried out AFM imaging. B.N. helped to direct the research and edit the manuscript. T.B. helped plan the experiments and prepare/edit the manuscript.

Acknowledgment. We gratefully acknowledge King Abdullah University of Science and Technology (KAUST) for a grant awarded to B. Nordén, and the U.K. BBSRC for the sLoLa grant to T. Brown. "Extending the boundaries of nucleic acid chemistry." Oligonucleotides were synthesised by ATDBio Ltd. We thank Dr. G. John Langley and Julie Herniman for supervision of the oligonucleotide mass spectrometry facility.

Supporting Information Available: Detailed descriptions of oligonucleotide design, synthesis, purification and characterisation, and nanostructure construction/fixation and deconstruction, and additional methods are given in the Supporting Information. This material is available free of charge via the Internet at http://pubs.acs.org.

REFERENCES AND NOTES

1. Bath, J.; Turberfield, A. J. DNA Nanomachines. *Nat. Nanotechnol.* **2007**, *2*, 275–284.
2. Feldkamp, U.; Niemeyer, C. M. Rational Design of DNA Nanoarchitectures. *Angew. Chem., Int. Ed.* **2006**, *45*, 1856–1876.
3. Rothemund, P. W. K. Folding DNA to Create Nanoscale Shapes and Patterns. *Nature* **2006**, *440*, 297–302.
4. Kuzuya, A.; Komiyama, M. DNA Origami: Fold, Stick, and Beyond. *Nanoscale* **2010**, *2*, 310–322.
5. Andersen, E. S.; Dong, M.; Nielsen, M. M.; Jahn, K.; Subramani, R.; Mamdouh, W.; Golas, M. M.; Sander, B.; Stark, H.; Oliveira, C. L. P.; *et al.* Self-Assembly of a Nanoscale DNA Box with a Controllable Lid. *Nature* **2009**, *459*, 73–76.
6. Tumpane, J.; Sandin, P.; Kumar, R.; Powers, V. E. C.; Lundberg, E. P.; Gale, N.; Baglioni, P.; Lehn, J.-M.; Albinsson, B.; Lincoln, P.; *et al.* Addressable High-Information-Density DNA Nanostructures. *Chem. Phys. Lett.* **2007**, *440*, 125–129.
7. Wang, D.; Kodali, V. K.; Underwood, W. D., II; Jarvholm, J. E.; Okada, T.; Jones, S. C.; Rumi, M.; Dai, Z.; King, W. P.; Marder, S. R.; *et al.* Thermochemical Nanolithography of Multifunctional Nanotemplates for Assembling Nano-Objects. *Adv. Funct. Mater.* **2009**, *19*, 3696–3702.
8. Koh, A. L.; Fernández-Domínguez, A. I.; McComb, D. W.; Maier, S. A.; Yang, J. K. W. High-Resolution Mapping of Electron-Beam-Excited Plasmon Modes in Lithographically Defined Gold Nanostructures. *Nano Lett.* **2011**, *11*, 1323–1330.
9. Liu, H.; Wang, B.; Ke, L.; Deng, J.; Chum, C. C.; Teo, S. L.; Shen, L.; Maier, S. A.; Teng, J. High Aspect Subdiffraction-Limit Photolithography *via* a Silver Superlens. *Nano Lett.* **2012**, *12*, 1549–1554.
10. Zhang, H.; Chung, S.-W.; Mirkin, C. A. Fabrication of Sub-50-nm Solid-State Nanostructures on the Basis of Dip-Pen Nanolithography. *Nano Lett.* **2003**, *3*, 43–45.
11. Salaita, K.; Wang, Y.; Mirkin, C. A. Applications of Dip-Pen Nanolithography. *Nat. Nano.* **2007**, *2*, 145–155.
12. Sandin, P.; Tumpane, J.; Borjesson, K.; Wilhelmsson, L. M.; Brown, T.; Nordén, B.; Albinsson, B.; Lincoln, P. Thermodynamic Aspects of DNA Nanoconstruct Stability and Design. *J. Phys. Chem. C* **2009**, *113*, 5941–5946.
13. Lundberg, E. P.; Plesa, C.; Wilhelmsson, L. M.; Lincoln, P.; Brown, T.; Nordén, B. Nanofabrication Yields. Hybridization and Click-Fixation of Polycyclic DNA Nanoassemblies. *ACS Nano* **2011**, *5*, 7565–7575.
14. Erben, C. M.; Goodman, R. P.; Turberfield, A. J. A Self-Assembled DNA Bipyramid. *J. Am. Chem. Soc.* **2007**, *129*, 6992–6993.
15. Goodman, R. P.; Schaap, A. T.; Tardin, C. F.; Erben, C. M.; Berry, R. M.; Schmidt, C. F.; Turberfield, A. J. Rapid Chiral Assembly of Rigid DNA Building Blocks for Molecular Nanofabrication. *Science* **2005**, *310*, 1661–1665.
16. Lundberg, E. P.; El-Sagheer, A. H.; Kočalka, P.; Wilhelmsson, L. M.; Brown, T.; Nordén, B. A New Fixation Strategy for Addressable Nano-Network Building Blocks. *Chem. Commun.* **2010**, 3714–3716.
17. Ohshiro, T.; Zako, T.; Watanabe-Tamaki, R.; Tanakab, T.; Maeda, M. A Facile Method Towards Cyclic Assembly of Gold Nanoparticles using DNA Template Alone. *Chem. Commun.* **2010**, 6132–6134.
18. Rajendran, A.; Endo, M.; Katsuda, Y.; Hidaka, K.; Sugiyama, H. Photo-Cross-Linking-Assisted Thermal Stability of DNA Origami Structures and Its Application for Higher-Temperature Self-Assembly. *J. Am. Chem. Soc.* **2011**, *133*, 14488–14491.
19. Spielmann, H. P.; Dwyer, T. J.; Hearst, J. E.; Wemmer, D. E. Solution Structures of Psoralen Monoadducted and Cross-Linked DNA Oligomers by NMR Spectroscopy and Restrained Molecular Dynamics. *Biochemistry* **1995**, *34*, 12937–12953.
20. Arslan, P.; Jyo, A.; Ihara, T. Reversible Circularization of an Anthracene-Modified DNA Conjugate through Bimolecular Triplex Formation and Its Analytical Application. *Org. Biomol. Chem.* **2010**, *8*, 4843–4848.
21. Ogasawara, S.; Fujimoto, K. A Novel Method to Synthesize Versatile Multiple-Branched DNA (MB-DNA) by Reversible

Photochemical Ligation. *ChemBioChem* **2005**, *6*, 1756–1760.
22. Fujimoto, K.; Yoshimura, Y.; Toba, S.; Nitta, Y. Light-Responsive Artificial Nucleoside having Photo-Crosslinking Ability. EP 2216338, August 11, 2010.
23. Yoshimura, Y.; Ohtake, T.; Okada, H.; Fujimoto, K. A New Approach for Reversible RNA Photocrosslinking Reaction: Application to Sequence-Specific RNA Selection. *ChemBioChem* **2009**, *10*, 1473–1476.
24. Yoshimura, Y.; Fujimoto, K. Ultrafast Reversible Photo-Cross-Linking Reaction: Toward *in Situ* DNA Manipulation. *Org. Lett.* **2008**, *10*, 3227–3230.
25. Fujimoto, K.; Yoshimura, Y. Sequence-Specific Nucleic Acid Purification Method Manner. U.S. 2011/0034683, February 10, 2011.
26. Fujimoto, K.; Hiratsuka-Konishi, K.; Sakamoto, T.; Yoshimura, Y. Site-Specific Photochemical RNA Editing. *Chem. Commun.* **2010**, 7545–7547.
27. Fujimoto, K.; Hiratsuka-Konishi, K.; Sakamoto, T.; Yoshimura, Y. Site-Specific Cytosine to Uracil Transition by Using Reversible DNA Photo-crosslinking. *ChemBioChem* **2010**, *11*, 1661–1664.
28. Fujimoto, K.; Hiratsuka-Konishi, K.; Sakamoto, T.; Ohtake, T.; Shinohara, K.-i.; Yoshimura, Y. Specific and Reversible Photochemical Labeling of Plasmid DNA using Photoresponsive Oligonucleotides Containing 3-Cyanovinylcarbazole. *Mol. BioSyst.* **2012**, *8*, 491–494.
29. Tagawa, M.; Shohda, K.-i.; Fujimoto, K.; Suyama, A. Stabilisation of DNA Nanostructures by Photo-Cross-Linking. *Soft Matter* **2011**, *7*, 10931–10934.
30. Yoshimura, Y.; Okada, H.; Fujimoto, K. Photoreversible DNA End Capping for the Formation of Hairpin Structures. *Org. Biomol. Chem.* **2010**, *8*, 1523–1526.
31. Jewett, J. C.; Sletten, E. M.; Bertozzi, C. R. Rapid Cu-Free Click Chemistry with Readily Synthesized Biarylazacyclooctynones. *J. Am. Chem. Soc.* **2010**, *132*, 3688–3690.
32. Aldaye, F. A.; Sleiman, H. F. Sequential Self-Assembly of a DNA Hexagon as a Template for the Organization of Gold Nanoparticles. *Angew. Chem., Int. Ed.* **2006**, *45*, 2204–2209.
33. Aldaye, F. A.; Sleiman, H. F. Guest-Mediated Access to a Single DNA Nanostructure from a Library of Multiple Assemblies. *J. Am. Chem. Soc.* **2007**, *129*, 10070–10071.
34. Aldaye, F. A.; Sleiman, H. F. Modular Access to Structurally Switchable 3D Discrete DNA Assemblies. *J. Am. Chem. Soc.* **2007**, *129*, 13376–13377.
35. Heuer, D. M.; Saha, S.; Archer, L. A. Topological Effects on the Electrophoretic Mobility of Rigid Rodlike DNA in Polyacrylamide Gels. *Biopolymers* **2003**, *70*, 471–481.
36. Mbua, N. E.; Guo, J.; Wolfert, M. A.; Steet, R.; Boons, G.-J. Strain-Promoted Alkyne−Azide Cycloadditions (SPAAC) Reveal New Features of Glycoconjugate Biosynthesis. *ChemBioChem* **2011**, *12*, 1912–1921.
37. Shelbourne, M.; Chen, X.; Brown, T.; El-Sagheer, A. H. Fast Copper-Free Click DNA Ligation by the Ring-Strain Promoted Alkyne-Azide Cycloaddition Reaction. *Chem. Commun.* **2011**, *47*, 6257–6259.
38. Agard, N. J.; Baskin, J. M.; Prescher, J. A.; Lo, A.; Bertozzi, C. R. A Comparative Study of Bioorthogonal Reactions with Azides. *ACS Chem. Biol.* **2006**, *1*, 644–648.
39. Shelbourne, M.; Brown, T., Jr; El-Sagheer, A. H.; Brown, T. Fast and Efficient DNA Crosslinking and Multiple Orthogonal Labelling by Copper-Free Click Chemistry. *Chem. Commun.* **2012**, 10.1039/C2CC35084J.
40. Moreno-Herrero, F.; Colchero, J.; Baró, A. M. DNA Height in Scanning Force Microscopy. *Ultramicroscopy* **2003**, *96*, 167–174.
41. Zhang, D. Y.; Seelig, G. Dynamic DNA Nanotechnology using Strand-Displacement Reactions. *Nat. Chem.* **2011**, *3*, 103–113.
42. Bath, J.; Green, S. J.; Allen, K. E.; Turberfield, A. J. Mechanism for a Directional, Processive and Reversible DNA Motor. *Small* **2009**, *5*, 1513–1516.
43. Chakraborty, B.; Sha, R.; Seeman, N. C. A DNA-Based Nanomechanical Device with Three Robust States. *Proc. Natl. Acad. Sci. U. S. A.* **2008**, *105*, 17245–17249.
44. He, Y.; Liu, D. R. Autonomous Multistep Organic Synthesis in a Single Isothermal Solution Mediated by a DNA Walker. *Nat. Nanotechnol.* **2010**, *5*, 778–782.
45. McKee, M. L.; Milnes, P. J.; Bath, J.; Stulz, E.; Turberfield, A. J.; O'Reilly, R. K. Multistep DNA-Templated Reactions for the Synthesis of Functional Sequence Controlled Oligomers. *Angew. Chem., Int. Ed.* **2010**, *49*, 7948–7951.
46. Di Felice, R.; Möller, R.; Festag, G.; Fritzsche, W.; Ingebrandt, S.; Offenhäusser, A. In *Nanobioelectronics - for Electronics, Biology, and Medicine*, 1st ed.; Offenhäusser, A.; Rinaldi, R., Eds.; Springer Science+Business Media, LLC: New York, 2009; Vol. XIV, pp 43−129.
47. Maune, H. T.; Han, S.-p.; Barish, R. D.; Bockrath, M.; Goddard, W. A., III; Rothemund, P. W. K.; Winfree, E. Self-Assembly of Carbon Nanotubes into Two-Dimensional Geometries using DNA Origami Templates. *Nat. Nanotechnol.* **2010**, *5*, 61–66.
48. Darby, R. A. J.; Sollogoub, M.; McKeen, C.; Brown, L.; Risitano, A.; Brown, N.; Barton, C.; Brown, T.; Fox, K. R. High Throughput Measurements of Duplex, Triplex and Quadruplex Melting Curves using Molecular Beacons and a LightCycler. *Nucleic Acids Res.* **2002**, *30*, e39.
49. Zipper, H.; Brunner, H.; Bernhagen, J.; Vitzthum, F. Investigations on DNA Intercalation and Surface Binding by SYBR Green I, its Structure Determination and Methodological Implications. *Nucleic Acids Res.* **2004**, *32*, e103.
50. Horcas, I.; Fernández, R.; Gómez-Rodríguez, J. M.; Colchero, J.; Gómez-Herrero, J.; Baró, A. M. WSXM: A Software for Scanning Probe Microscopy and a Tool for Nanotechnology. *Rev. Sci. Instrum.* **2007**, *78*, 013705.